

Prediction of Fatigue Crack Propagation Behavior from a Pre-Crack under Combined Torsional and Axial Loadings

Keisuke TANAKA¹, Takuya KATO¹ and Yoshiaki AKINIWA¹

¹ Department of Mechanical Engineering, Nagoya University, Nagoya 464-8603, Japan
ktanaka@mech.nagoya-u.ac.jp

ABSTRACT. *The fatigue crack propagation behavior from a pre-crack under cyclic torsion combined with static or cyclic axial loading was predicted on the basis of the maximum tangential stress criterion. The prediction was compared with the experimental results obtained for thin-walled tubular specimens made of a medium carbon steel. The direction of fatigue crack propagation follows the direction of the maximum of the total range of the tangential stress, $\Delta\sigma_{\theta \max}$, near the crack tip and then gradually changes to the direction perpendicular to the maximum of the total range of the principal nominal stress. The mode II stress intensity factor range quickly gets close to zero after a small amount of crack extension. The propagation rate was faster than the uniaxial data as cracks extended a long distance.*

INTRODUCTION

Fatigue fracture of several engineering components such as transmission shafts, pipes and suspension coil springs occurs under combined torsional and axial loading. For damage tolerance design, the direction as well as the rate of crack propagation should be predicted from loading conditions and material inhomogeneities. In the present paper, the predictions of fatigue crack propagation direction and rate from a pre-crack were performed on an isolated crack under cyclic shear combined with static or cyclic tension, and compared with the experimental data on crack propagation from a pre-crack in thin-walled tubular specimens made of a medium-carbon steel subjected to cyclic torsion combined with static or cyclic tension [1].

PROCEDURE OF PREDICTION

Analytical Model and Fatigue Conditions

An infinite plate with a pre-crack under tensile and shear stresses was analyzed as shown in Fig. 1. The total length of a pre-crack was 1 mm. The origin of the coordinates was taken at the center of the pre-crack and the angle of crack extension was measured counter clockwise with respect to the horizontal (circumferential) direction (see Fig. 1). The curvature effect of thin-walled tubes on the stress intensity factor (SIF) was not taken into account in the analysis.

The direction of fatigue crack propagation was predicted by the maximum tangential

stress criterion. The SIF value was computed by using the two-dimensional body force method (BFM). The predictions of the crack propagation path and rate were compared with the experimental results of pre-cracked thin-walled tubular specimens made of a medium carbon steel (JIS S45C) subjected to cyclic torsion combined with static or cyclic tension. The chemical compositions of the material were as follows (mass.%) : C0.43, Si0.19, Mn0.81, P0.022, Cu0.01, Ni0.02, Cr0.14. The mechanical properties of the material was as follows : the yield strength was 319 MPa, the tensile strength was 583 MPa, Young's modulus was 216 GPa, and Poisson's ratio was 0.279.

The fatigue test conditions are four cases. The stress ratio of cyclic torsion is $R=-1$ for all cases. A static axial stress is superposed on cyclic torsion in cases B and C. For case D, cyclic axial loading is superposed in-phase with cyclic torsion.

Maximum Tangential Stress Criterion

Three versions of the maximum tangential stress criterion were used for predictions.

Criterion I: $\Delta\sigma_{\theta \max}$ criterion

$\Delta\sigma_{\theta \max}$ criterion assumes the direction of crack extension coincident with the direction perpendicular to the maximum of the total range of the tangential stress including the negative stress at the crack tip. Under cyclic torsion with superposed static and cyclic axial loading, the maximum SIF values for mode I and II, $K_{I \max}$ and $K_{II \max}$, are given as the sum of those of static components, K_{Is} and K_{IIs} , and of cyclic components, K_{Ia} and K_{IIa} , as follows:

$$K_{I \max} = K_{Is} + K_{Ia} \quad (1)$$

$$K_{II \max} = K_{IIs} + K_{IIa} \quad (2)$$

The tangential stress σ^+_{θ} near the crack tip at the maximum load is defined as

$$\sigma^+_{\theta} = \frac{K_{Is} + K_{Ia}}{\sqrt{2\pi r}} \cos^3\left(\frac{\theta}{2}\right) - 3 \frac{K_{IIs} + K_{IIa}}{\sqrt{2\pi r}} \cos^2\left(\frac{\theta}{2}\right) \sin\left(\frac{\theta}{2}\right) \quad (3)$$

where r and θ are the local coordinates near the crack tip. When the contact of crack faces is neglected, the tangential σ^-_{θ} at the minimum load is

$$\sigma^-_{\theta} = \frac{K_{Is} - K_{Ia}}{\sqrt{2\pi r}} \cos^3\left(\frac{\theta}{2}\right) - 3 \frac{K_{IIs} - K_{IIa}}{\sqrt{2\pi r}} \cos^2\left(\frac{\theta}{2}\right) \sin\left(\frac{\theta}{2}\right) \quad (4)$$

The range of the tangential stress, $\Delta\sigma_{\theta}$, can be written as follows :

$$\Delta\sigma_{\theta} = \left| \frac{\Delta K_I}{\sqrt{2\pi r}} \cos^3\left(\frac{\theta}{2}\right) - 3 \frac{\Delta K_{II}}{\sqrt{2\pi r}} \cos^2\left(\frac{\theta}{2}\right) \sin\left(\frac{\theta}{2}\right) \right| \quad (5)$$

where $\Delta K_I = 2K_{Ia}$ and $\Delta K_{II} = 2K_{IIa}$. The direction of the maximum tangential stress is given by

$$\Delta K_I \sin \theta + \Delta K_{II} (3 \cos \theta - 1) = 0 \quad (6)$$

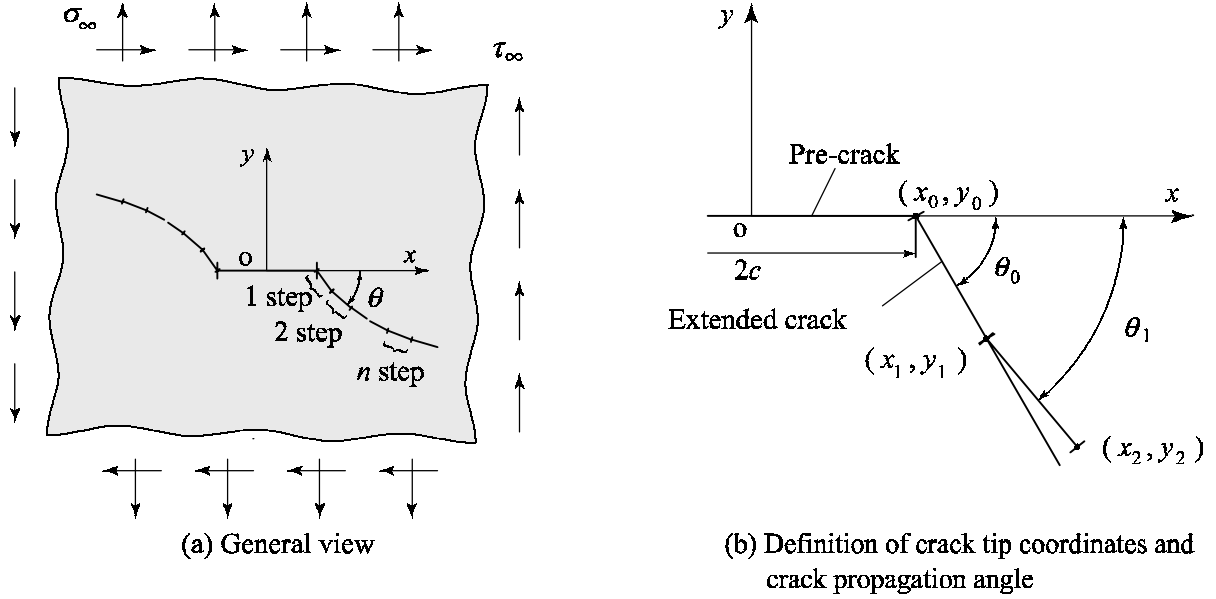


Figure 1. BFM model for crack propagation in infinite plate under tensile and shear stress.

Criterion II: $\Delta\sigma^+_{\theta_{max}}$ criterion

For fatigue crack propagation, only the tensile part of the cyclic stress can be effective. $\Delta\sigma^+_{\theta_{max}}$ criterion assumes the direction of crack propagation coincident with the direction perpendicular to the maximum of the positive range of the tangential stress at the crack tip. By using the notations of Eqs (3) and (4), $\Delta\sigma^+_{\theta}$ can be written as

$$\Delta\sigma^+_{\theta} = \left| \sigma^+_{\theta} - \max(\sigma^-_{\theta}, 0) \right| \quad (7)$$

The crack propagation direction is assumed to be perpendicular to the direction of the maximum of $\Delta\sigma^+_{\theta}$.

Criterion III: $\Delta\sigma^*_{\theta_{max}}$ criterion

Under reverse loading, crack surfaces may come into contact with each other. When crack-face contact takes place, the SIF value at the minimum load is different from the nominal value calculated from the applied load. By taking into account of crack-face contact, the minimum value of SIF was calculated by BFM and is denoted by K^*_{min} . The range of SIF is expressed by

$$\Delta K^* = K_{max} - K^*_{min} \quad (8)$$

The crack tip was closed under the minimum load for all cases of the experiments. The mode I component $K^*_{I_{min}}$ is zero, so $\Delta K^*_I = K_{I_{max}}$. On the other hand, the mode II component $K^*_{II_{min}}$ is not zero. The range of the tangential stress and the crack direction are calculated by substituting ΔK^*_I and ΔK^*_{II} for ΔK_I and ΔK_{II} in Eqs (5) and (6), respectively.

Crack Propagation Rate

The relation between the fatigue crack propagation rate, da/dN (m/cycle), and the maximum stress intensity factor, $K_{I\max}$ (MPa), of the experimental material was reported by Zhang et al. [2] for the case of the stress ratio $R=-1$. The crack propagation law is expressed as

$$da / dN = C (K_{I\max})^m \quad (9)$$

where $C = 1.76 \times 10^{-12}$ and $m = 3.69$. The threshold value is $K_{I\max\text{th}} = 5.26 \text{ MPa}\sqrt{\text{m}}$. The maximum stress intensity factor, $k_{I\max}$, for a small kink of the main crack is equal to

$$K_{I\max} = \sigma_{\theta} \sqrt{2\pi r} = K_{I\max} \cos^3\left(\frac{\theta}{2}\right) - 3K_{II\max} \cos^2\left(\frac{\theta}{2}\right) \sin\left(\frac{\theta}{2}\right) \quad (10)$$

where θ is the angle of crack, and K_I and K_{II} are the maximum SIF values for the main crack. By substituting $k_{I\max}$ for $K_{I\max}$ in Eq. (9), the crack propagation rate can be obtained.

In the simulation of crack propagation, the increment of crack length for one step is determined by

$$\Delta a = (da / dN) \times N \quad (11)$$

where $N=10000$ cycle.

COMPARISON WITH EXPERIMENTAL RESULTS

Crack Propagation Path and Angle

The crack propagation path was traced in SEM micrographs in order to make a comparison with the predicted path. Figure 2 shows the traced paths and predicted paths for four cases. In prediction, the $\Delta\sigma_{\theta\max}$ and $\Delta\sigma^+_{\theta\max}$ criteria yield the identical path for case A, while $\Delta\sigma^*_{\theta\max}$ criterion gives a slightly different path. For cases B and C, the crack paths predicted by the three criteria are all different. For case D, the crack paths predicted by the three criteria are nearly identical. The crack paths predicted by $\Delta\sigma^*_{\theta\max}$ criterion for case A, B, and C are slightly different from those by $\Delta\sigma_{\theta\max}$ criterion because of the existence of ΔK^*_{II} value. The crack propagation path predicted by $\Delta\sigma^*_{\theta\max}$ criterion is the closest to the experimental results, although there is a slight difference in the initial stage of crack extension from a pre-crack.

Since the crack propagation path is zigzag under the influence of the material microstructure, the crack path was approximated by a curve of the second order and the angle was measured for the approximated crack path. Figure 3 shows the change of the crack propagation angle with crack extension. The difference of the crack propagation angles predicted by $\Delta\sigma_{\theta\max}$ and $\Delta\sigma^*_{\theta\max}$ criteria becomes minimal as the crack extends.

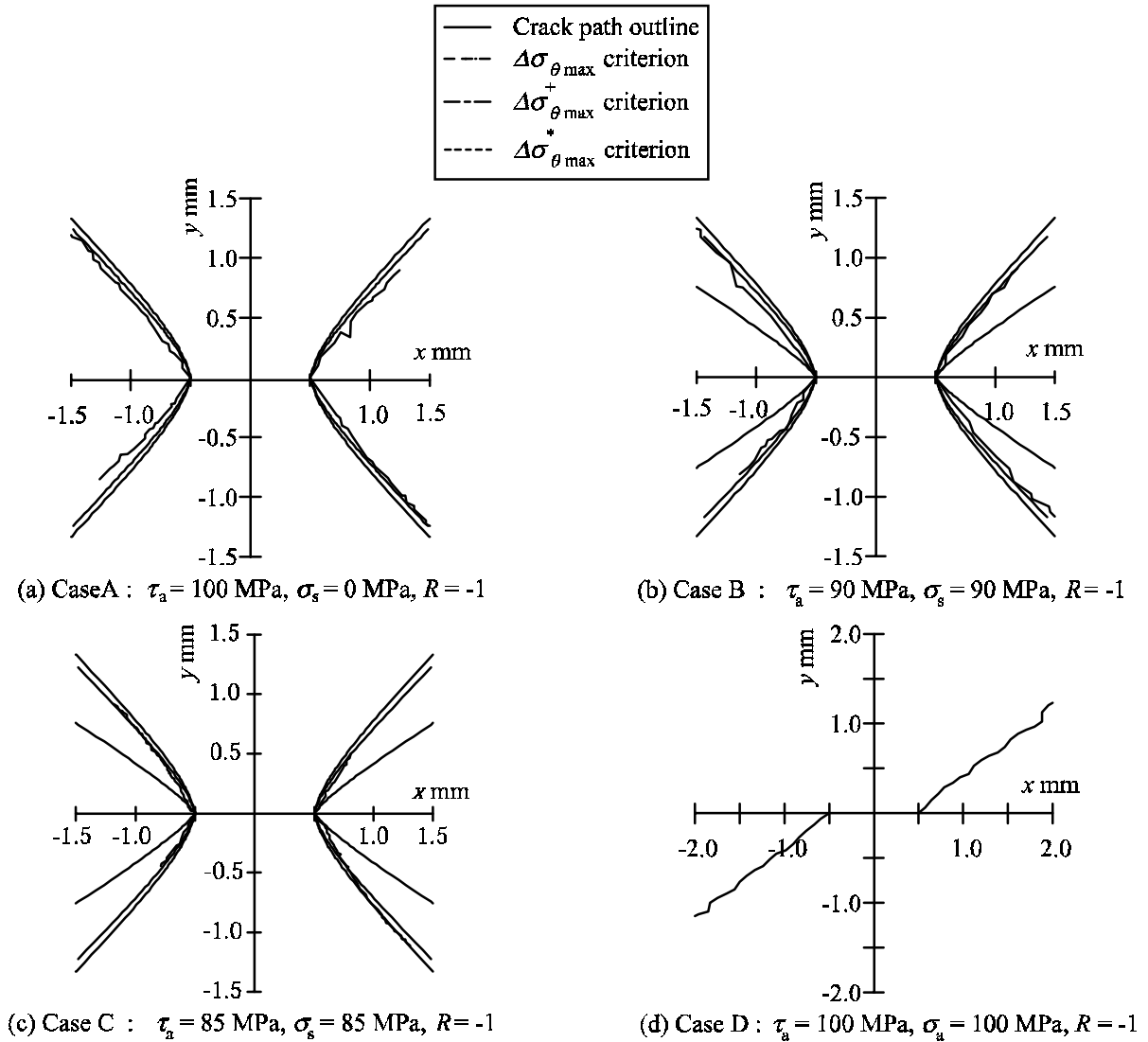


Figure 2. Crack path outline and the predicted propagation path.

Only for cases B and C, the prediction based on $\Delta\sigma_{\theta_{\max}}^+$ criterion is much different from that based on $\Delta\sigma_{\theta_{\max}}$ and $\Delta\sigma_{\theta_{\max}}^*$ criteria. It should be noted that $\Delta\sigma_{\theta_{\max}}$ and $\Delta\sigma_{\theta_{\max}}^*$ criteria give a better prediction of the crack propagation angle than $\Delta\sigma_{\theta_{\max}}^+$ criterion. At short lengths of crack extension up to about 0.2 mm, the experimental angle is smaller than the predicted angles based on $\Delta\sigma_{\theta_{\max}}$ and $\Delta\sigma_{\theta_{\max}}^*$ criteria. This difference may come from the difference of the crack front shape within the specimen thickness.

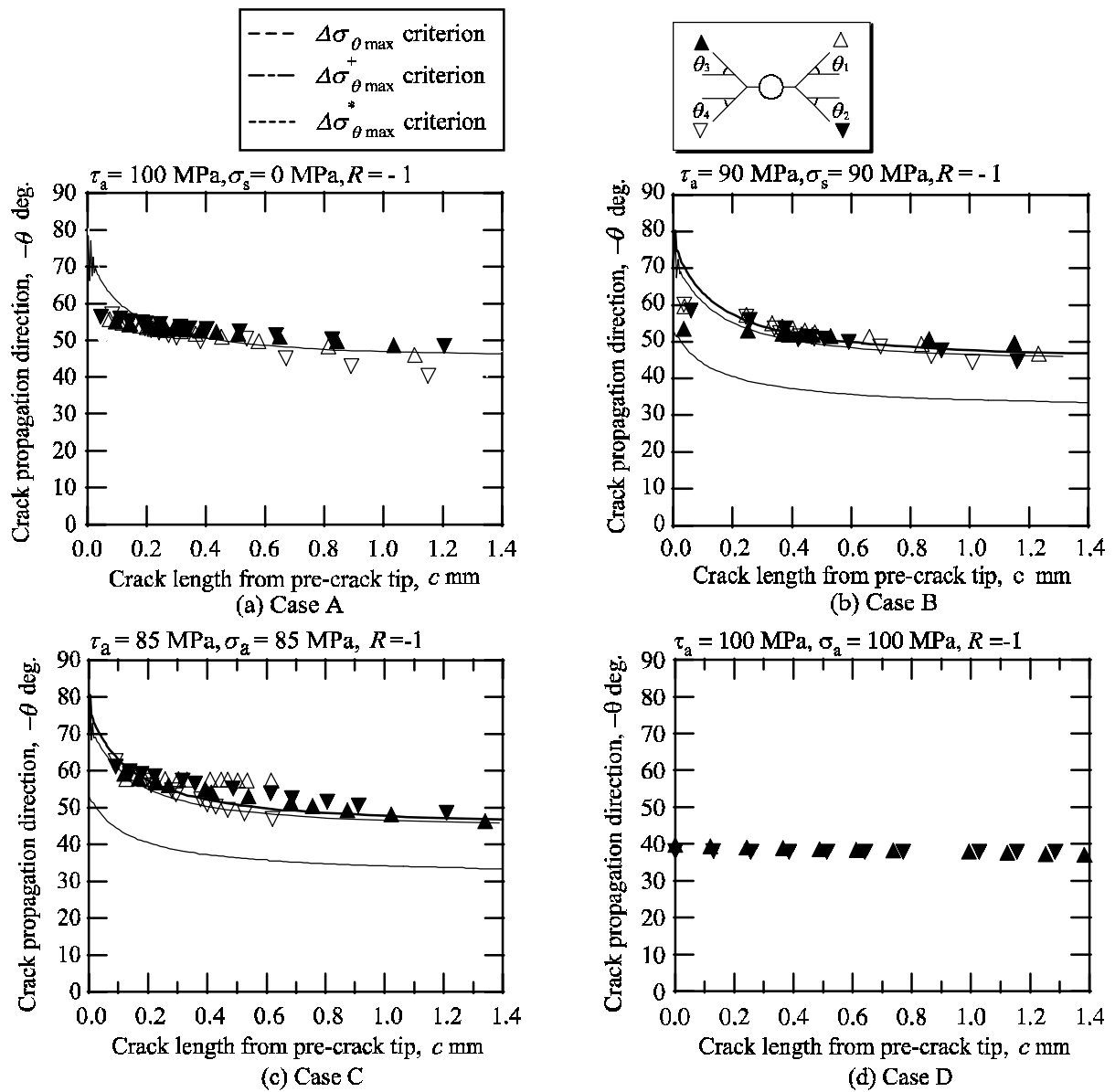


Figure 3. Fatigue crack propagation direction.

Stress Intensity Factor

The SIF value for kinked cracks was calculated by using BFM. The calculation was performed for predicted and experimentally-traced cracks under the plane stress condition. For the case of combination of torsional and tensile loadings, the SIF value was obtained as the sum of two loadings. Under a positive shear stress, the crack kinks at the upper right and lower left are closed (see Fig. 1 or 2), so only crack kinks at the

upper left and lower right are modeled in calculation. On the other hand, under a negative shear stress, only crack kinks at the upper left and lower right are modeled. The number of division of a pre-crack is 100 and that for extended kinks is 10.

Figure 4 shows the maximum SIF values for experimentally-traced cracks and predicted cracks by $\Delta\sigma_{\theta_{\max}}$ and $\Delta\sigma^*_{\theta_{\max}}$, where the maximum SIF values for the upper right and lower left kinks take place at the positive shear stress, and those for the upper left and lower right kinks at the negative shear stress. For case A, the mode II SIF values quickly get close to zero as the crack extends, while the mode I SIF is a monotonically increasing function. For case B, the mode II SIF is not reduced to zero even at long crack extensions. The mode II components are induced mainly by a static tensile stress.

Figure 5 shows the change of the range of SIF values for case B. The ΔK_I and ΔK^*_I values increase monotonically with crack extension. The ranges of mode II SIF, ΔK_{II} and ΔK^*_{II} are reduced to zero as cracks extend. While the prediction gives zero to ΔK_{II} and ΔK^*_{II} just after crack extension, the experimental results show a gradual reduction of the mode II component. When the crack length is longer than about 0.2 mm, the ΔK_{II} value is nearly zero in the experimentally-traced crack paths. Therefore, it can be said that the direction of crack path follows the direction in which the cyclic component of mode II SIF is zero.

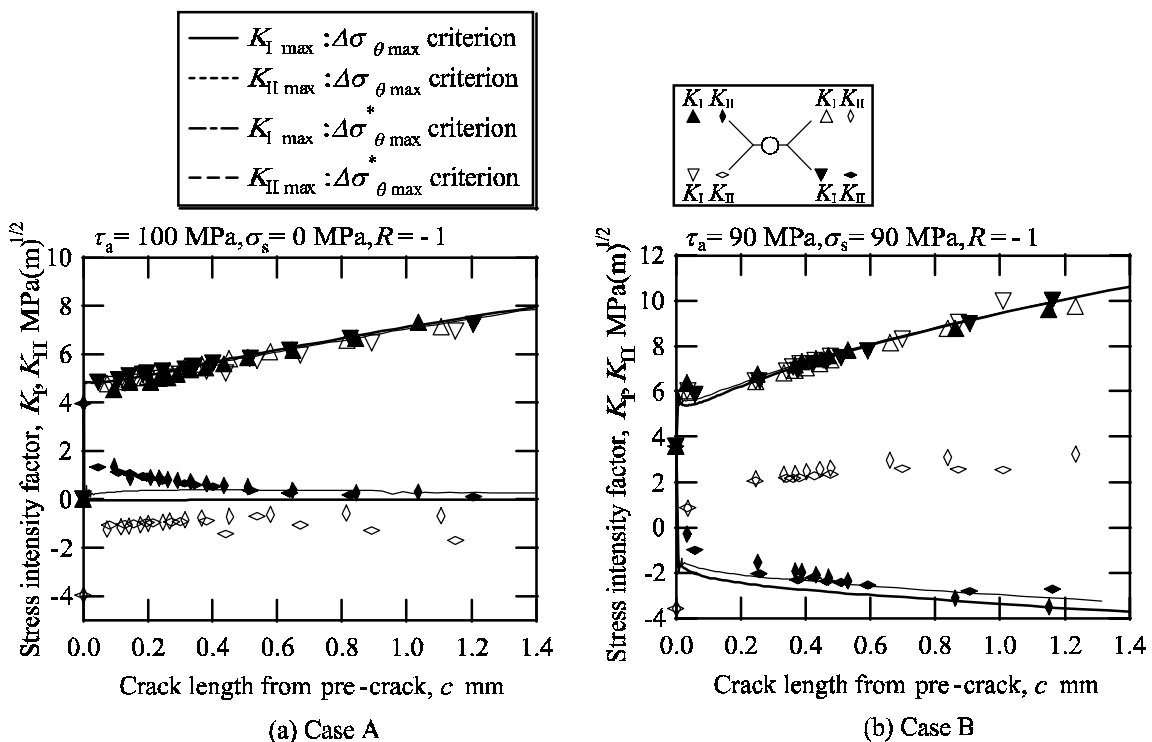


Figure 4. Change of maximum stress intensity factor with crack length.

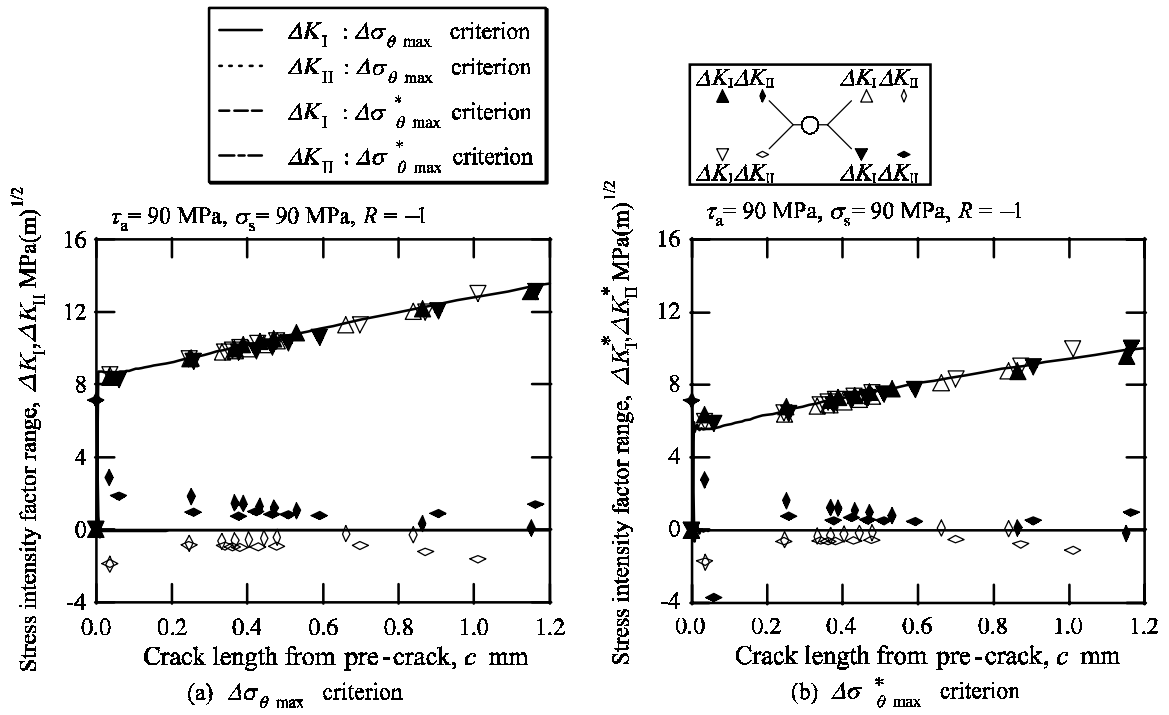


Figure 5. Change of stress intensity factor range with crack extension (Case B).

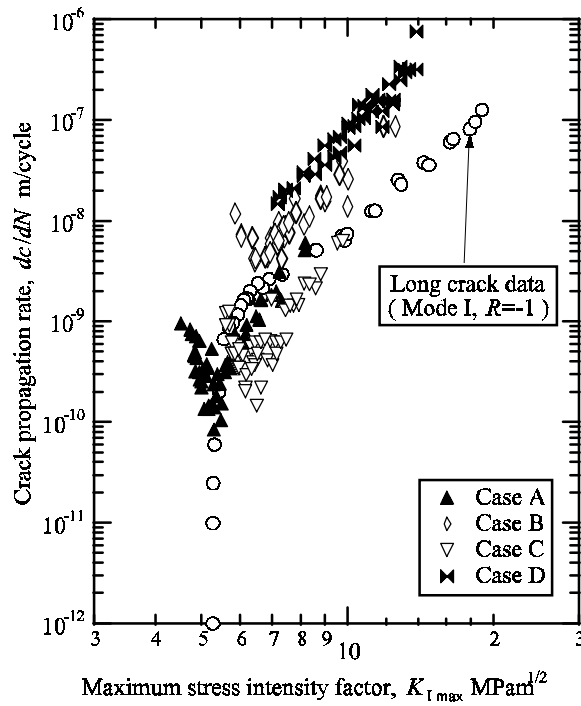


Figure 6. Relation between crack propagation rate and maximum stress intensity factor.

Crack Propagation Rate

The relation between the rate of fatigue crack propagation, dc/dN , and the maximum value of mode I SIF value, $K_{I\max}$, determined in the previous section from experimentally-traced paths is shown in Figure 6, where the data of the relation for long cracks under uniaxial loading are also shown with the open circles. For case A, the propagation rate decreases in the initial stage and then increases with crack extension. A similar tendency is seen for cases B and C. As the crack length gets longer, the crack propagation rate becomes higher than the uniaxial data as typically seen for case B. For case D, there is no dip in the crack propagation behavior. The crack propagation rate is much higher than the uniaxial data.

The initial dip of the crack propagation behavior is caused by the development crack closure, and will be studied in the future. Higher propagation rates above the uniaxial data observed in cases B and D result from the excessive plasticity due to negative non-singular T stress. The J integral approach was proved to be an appropriate parameter for these cases [3].

CONCLUSIONS

The predictions of the crack propagation path and rate based on the maximum tangential stress criterion were compared with the previous fatigue tests of crack propagation from a pre-crack in thin-walled tubular specimens made of a medium-carbon steel subjected cyclic torsion with and without superposed static and cyclic axial loading. The results were summarized as follows:

- (1) Fatigue cracks propagate in the direction of the maximum of the total range of the tangential stress, $\Delta\sigma_{\theta\max}$, near the crack tip and then gradually changes to the direction perpendicular to the maximum of the total range of the principal nominal stress.
- (2) The stress intensity factor of a kink crack from a pre-crack or a main crack is calculated by using BFM. The mode II stress intensity factor range ΔK_{II} quickly gets close to zero after small amount of crack extension.
- (3) The crack propagation rate decreases first and then increases with crack extension. This dip of the crack propagation behavior is caused by the development of crack closure with crack extension.
- (4) As cracks extend, the propagation rate is faster than the uniaxial data when compared at the same stress intensity range. The negative nonsingular stress induces excessive plasticity ahead of the fatigue crack tip, and then accelerates fatigue crack propagation.

REFERENCES

1. Tanaka, K., Akiniwa, Y., Mikuriya, T., and Tanaka, Ko. (2001) *Trans. Jpn Soci. Mech. Engrs*, A-67, 2032-2038.

2. Zhang, L. M., Akiniwa, Y. and Tanaka, K. (1998) *Trans. Jpn Soci. Mech. Engrs*, A-64, 1229-1235.
3. Tanaka, K., Akiniwa, Y., Takahashi, A., and Mikuriya, T. (2002) In *Fatigue 2002*, pp. 1881-1888, Blom, A.F. (Ed), Engineering Materials Advisory Services Ltd., Apollo House, Redall Hill Road, Cradley Heath, West Midlands B64 5JT, U.K.